

Optically trapped probes with nanometer-scale tips for femto-Newton force measurement

To cite this article: M R Pollard *et al* 2010 *New J. Phys.* **12** 113056

View the [article online](#) for updates and enhancements.

Related content

- [Optical trapping and binding](#)
Richard W Bowman and Miles J Padgett
- [Probing the Casimir force with optical tweezers](#)
D. S. Ether jr., L. B. Pires, S. Umrath *et al.*
- [Single metal nanoparticles](#)
P Zijlstra and M Orrit

Recent citations

- [A single large assembly with dynamically fluctuating swarms of gold nanoparticles formed by trapping laser](#)
Tetsuhiro Kudo *et al*
- [Nanoscale Optical Trapping: A Review](#)
Carlo Bradac
- [Multibeam interferometric optical tweezers](#)
Mohammadbagher Mohammadnezhad and Abdollah Hassanzadeh



IOP | ebooks™

Bringing you innovative digital publishing with leading voices to create your essential collection of books in STEM research.

Start exploring the collection - download the first chapter of every title for free.

Optically trapped probes with nanometer-scale tips for femto-Newton force measurement

M R Pollard¹, S W Botchway¹, B Chichkov⁴, E Freeman²,
R N J Halsall², D W K Jenkins³, I Loader³, A Ovsianikov⁴,
A W Parker¹, R Stevens³, R Turchetta², A D Ward¹ and
M Towrie^{1,5}

¹ Central Laser Facility, Research Complex at Harwell, Science and Technology Facilities Council, Rutherford Appleton Laboratory, Didcot OX11 0FA, UK

² Technology Department, Science and Technology Facilities Council, Rutherford Appleton Laboratory, Didcot OX11 0QX, UK

³ Micro and Nanotechnology Centre, Science and Technology Facilities Council, Rutherford Appleton Laboratory, Didcot OX11 0QX, UK

⁴ Laser Zentrum Hannover e.V. Nanotechnology Department, Hollerithallee 8, 30419 Hannover, Germany

E-mail: mike.towrie@stfc.ac.uk

New Journal of Physics **12** (2010) 113056 (14pp)


Received 21 May 2010

Published 30 November 2010

Online at <http://www.njp.org/>

doi:10.1088/1367-2630/12/11/113056

Abstract. We describe the development of a novel force probe, controlled by multiple optical traps, with a nanometer-scale tip that protrudes outside the direct laser radiation field. We have measured forces to an accuracy of 240 fN, which enables future experiments that probe photo-sensitive components (such as biological cells) and non-transparent objects. The probes were produced using two methods, electron beam lithography and two-photon polymerization, with the latter providing approximately twice as much trapping stiffness.

 Online supplementary data available from stacks.iop.org/NJP/12/113056/mmedia

⁵ Author to whom any correspondence should be addressed.

Contents

1. Introduction	2
2. Method	3
2.1. Probe production	3
2.2. Optical trapping apparatus	5
3. Results	6
3.1. Characterization of optically trapped probes	6
3.2. Force measurement	9
4. Conclusions	12
Acknowledgments	12
References	13

1. Introduction

A major requirement in the investigation of the complex and dynamic processes that occur within living cells is the control and measurement of extremely small forces, < 1 pN (10^{-12} N). Several competing force measurement techniques exist, including atomic force microscopy, magnetic trapping and optical trapping [1]. Optical trapping has the unique capability to fulfill the need for manipulating single-molecule particles within biological environments to nanometer accuracy [2] and with femto-Newton (fN) force sensitivity [3].

Established optical trapping techniques have used micrometer-scale polystyrene spheres that were attached chemically to proteins in order to characterize the folding of ribonucleic acid (RNA) [4] and measure the chemical-to-mechanical energy conversion processes of motor proteins (e.g. kinesin and myosin) [5]–[7]. Smaller optically trapped force probes have been developed, such as gold nano-rods [8] and single-walled nano-tubes [9], and these can potentially measure fN forces (10^{-15} N) when applied in the axial direction. However, all these techniques suffer from a common problem—the exposure of the sample to the intense trapping light, which may lead to optical damage [10]. Additionally, for optically trapped probes smaller than 100 nm, difficulties arise in the control of their position and in their observation using microscopes and visible light sources [1].

With the aim of overcoming these limitations in fN force measurement, we have developed a force probe with a nanometer-scale tip connected to a microstructure that is easy to manipulate, held firmly in the microscope specimen plane and imaged using bright-field microscopy. Our design permits force measurement with improved spatial resolution beyond the influence of the trapping laser fields. Previous studies have produced complex, optically trapped probes by a variety of techniques including the manual assembly of coated silicon spheres connected to cadmium-sulfide rods [11]. Here, we describe two automated production methods, electron beam lithography (EBL) and two-photon polymerization (2PP), capable of producing large quantities of probes with nanometer-scale tips in a reliable fashion. The 2PP process has been successfully applied in the past to produce structures suitable for optical trapping [12, 13]. The EBL process that we employed could only produce structures with sharp edges (such as cylinders), which has known implications for the trapping stability, as identified in earlier studies [14, 15].

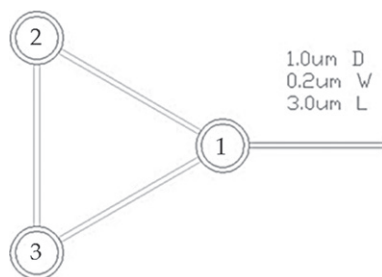


Figure 1. The probe design showing a triangular arrangement of the trapping points (numbered from 1 to 3) and a protruding tip. Typical cylinder dimensions are shown in top right.

2. Method

2.1. Probe production

The probe design [16] was based on a triangle that was optically trapped at each of its three corners, with a distinct force sensing arm equipped with a nanometer-scale tip that protruded from one of the corners, as shown in figure 1. The first fabrication of the probes used EBL to demonstrate the principle of creating this structure with a nanometer-scale gold tip. The probes were constructed using an electron-beam lithographic system (VB6-HR working at 100 keV) that had a writing resolution of 20 nm on a resist layer of SU8. The probe tips, made from gold and 50 nm wide by 1 μm long, were deposited onto the surface of the silicon wafer using a high-resolution mask that was written using EBL and a two-layer lift-off method (one layer of methyl methacrylate, 0.7 μm thick, followed by a second layer of poly(methyl methacrylate) of 0.3 μm thickness, supplied by MicroChem Corporation, NANO 950 PMMA A4). A layer of SU8 epoxy resin was spun on top of the silicon wafer and was selectively exposed using EBL to produce thousands of repeatable structures, as shown in figure 2(a) and in close-up in figure 2(b). A sacrificial layer of chrome, which was deposited at the start of the process between the silicon wafer and the SU8 layers, was removed using a 15 μl droplet of chrome etchant. The etching process released the probes into the droplet, which was further diluted using two 20 : 1 water dilutions. Due to the planar nature of the EBL technique (i.e. top-down), the triangular probes were produced with one cylindrical structure positioned at each of the three trapping points. A range of EBL probes were produced with cylinder dimensions of between 2 and 4 μm to investigate the effect of optical traps on cylindrical shapes, following on from previous modeling studies [13].

An alternative method using 2PP was investigated in order to produce probes with spherical trapping points. The 2PP technique produced probes with spherical nodes that were 4 μm in diameter and arranged in a triangular formation, and one tapered tip that was 5 μm long and had a minimum width of 200 nm. In contrast to the EBL process, the 2PP probes were produced as free-standing structures with two thin supporting feet to ensure the lowest possible contact area between the probe and the surface of the conventional glass cover slip onto which it was produced. Automated production of the probes was performed directly from computer-aided designs in the stereolithography format (STL), as shown in figure 3(a). The two-photon polymerization process used a material consisting of 20 : 80 zirconium–silicon sol–gel, containing 0.5% of 4,4'-bis(diethylaminobenzophenone) as a photo-initiator. This material is

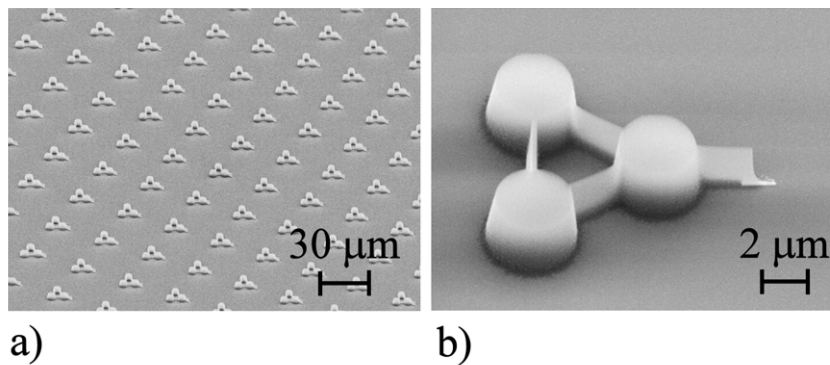


Figure 2. (a) Scanning electron micrograph (SEM) image of an array of probes produced using EBL. (b) SEM image of an EBL probe with its gold tip (50 nm wide by 1 μm long) held at a distance of 2 μm from the trapped structure, and distinctive cylindrical trapping points (3 μm wide by 3 μm high).

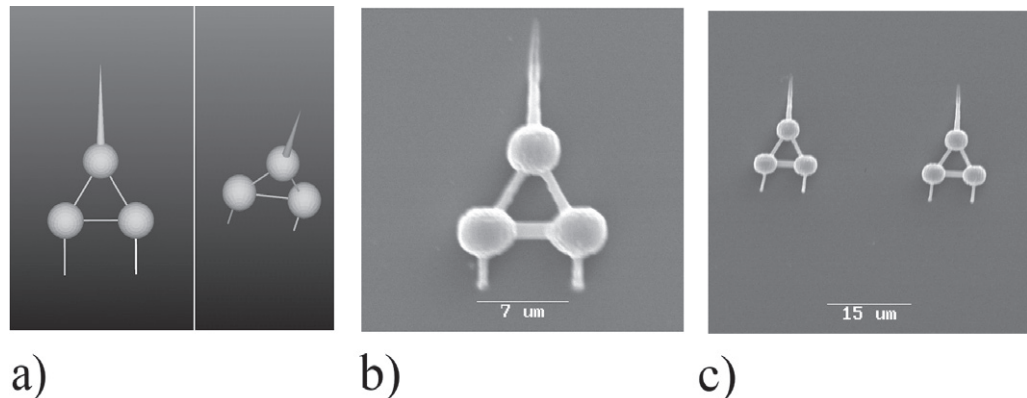


Figure 3. Free-standing probe fabricated by the 2PP technique: (a) original computer-aided design; (b, c) SEM images of representative structures. The tapered probe tip had a width of 200 nm.

characterized by a superior 2PP process and low shrinkage. Samples were prepared by drop casting the solution onto the glass coverslips, and prebaking them at 100 $^{\circ}\text{C}$ for 1 h, to form a hard gel. The structures were fabricated pointing upwards (i.e. out of the coverslip), with a slicing distance of 200 nm between the layers and a hatching distance of 200 nm within each layer. Examples of the probes are shown in figures 3(b) and (c). The scanning speed was set to 100 $\mu\text{m s}^{-1}$, while the average laser power, measured before focusing lens, was set to 45 mW for the structures shown in figures 3(b) and (c). The 2PP apparatus included a microscope fitted with a 100 \times objective lens (Zeiss, Plan Apochromat, numerical aperture of 1.4) to focus radiation of a pulsed laser (titanium–sapphire source, operated at 120 fs pulse duration, 90 MHz repetition rate and wavelength of 780 nm) into the volume of the sol–gel material. To remove the unpolymersed material, the structures were developed in 1-propanol. The extensive description of the experimental setup and the applied materials can be found elsewhere [17]. The probe structures were physically separated from the coverslip by placing the assembly in an ultrasonic bath. The 2PP probes were dried flat onto coverslips and later

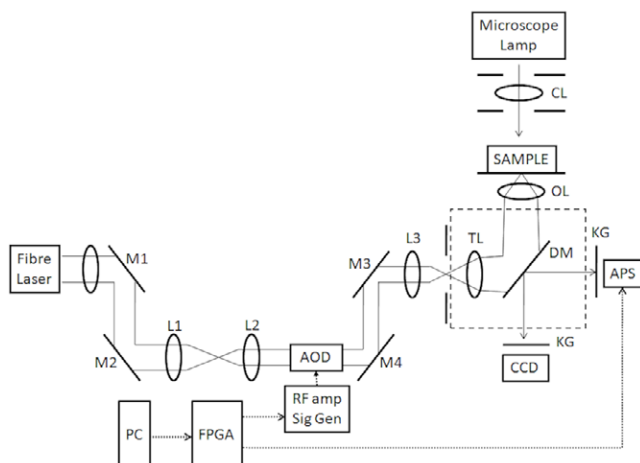


Figure 4. Optical trapping apparatus schematic, showing the trapping laser beam steering and shaping using mirrors (M1–M4), lenses (L1–L3) and acousto-optic deflector (AOD; Isle Optics TS100-XY), coupling into a microscope (shown as dotted line) via a tube lens (TL) and objective lens (OL) into the sample. Position measurement of the optically trapped probe was achieved using an APS and the microscope’s field of view was viewed separately using a CCD. The microscope lamp (100 W) was used to illuminate the sample. The dichroic mirror (DM) was used to reflect laser light to the sample and transmit visible light (shown as arrows) to APS and CCD with KG filters fitted to block laser light. Imaging was adjusted by using the condenser lens (CL) and diaphragms immediately above and below. A combination of a user computer (PC) and dedicated electronics (known as a field programmable gate array, FPGA) provides the control signals (shown as dotted arrows) to the AOD drive system (RF amplifier and signal generator) and to the APS.

released from the coverslip by creating an acoustic shock wave in the vicinity of the probe through the plasma breakdown of water induced by focusing a pulsed laser beam (with duration of < 1 ns, wavelength of 1064 nm and $10 \mu\text{J}$ of energy) through the microscope objective. This released the probe, without damage, into the solution for capture and manipulation by the optical traps.

2.2. Optical trapping apparatus

Each probe was trapped using three gradient optical traps [2] created by the rapid repositioning of a single laser beam at a rate of 40 kHz [18]. Up to three additional optical traps could be produced using the same laser beam for target manipulation. Our optical trapping apparatus (shown in figure 4) included an inverted microscope (Olympus IX70) with a $60\times$ water immersion objective lens (with numerical aperture of 1.2), a fiber laser light source with a wavelength of 1090 nm and an acousto-optic deflector (AOD) to reposition the laser beam (a full description is given in [19]). The instrumentation permitted two-dimensional control of the optically trapped probe with coarse axial control provided by the microscope focus. The size of the diffraction-limited focal spot of the trapping laser beam was calculated to be 450 nm [20].

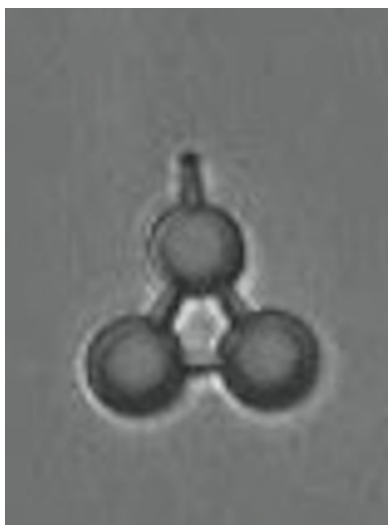


Figure 5. Manipulation of optically trapped probe produced using EBL with movement in continuous steps (see movie 1, available from stacks.iop.org/NJP/12/113056/mmedia).

The distance between the probe's trapping field and its tip was greater than $3\ \mu\text{m}$. Previous research had identified that at this distance there was no significant effect on nearby objects (and hence force measurement) due to the trapping field in this particular direction [21].

The force applied to the probe tip is derived using Hooke's law [1] and the correlated position measurements of the probe microstructure using visible-light images taken with an active pixel sensor (APS) [22, 23]. The three probe trapping points were imaged in individual regions of interest (ROIs), subsets of the APS image [19] that were recorded at a rate of 15 kHz. The position of each trapping point in the image plane was calculated using two center of mass calculations [24]; no position measurements for the probe in the axial direction were made. Three additional ROIs were used to measure the positions of the probe's target for test and force calibration purposes. Dedicated electronics operating at 100 MHz (known as a field programmable gate array or FPGA) were used to control the APS and AOD.

3. Results

3.1. Characterization of optically trapped probes

Individual probes were released into a sample container with a glass coverslip base (no. 1 thickness, $0.14\ \mu\text{m}$) and subsequently located, trapped and manipulated as shown in figures 5 and 6 for the EBL and 2PP probes, respectively. The probe and its surroundings were observed using a charge-coupled device (CCD) that viewed the microscope image plane. A range of EBL probes were tested, where the diameter of its three cylindrical trapping points was varied from 2 to $4\ \mu\text{m}$ and the height kept constant at $4\ \mu\text{m}$. Trapping of the EBL probes was problematic and only the $4\ \mu\text{m}$ size cylinders could be trapped in a stable and reliable fashion. Consequently, all further tests were carried out using this probe size. In contrast, the 2PP probes with spherical trapping points were trapped with relative ease.

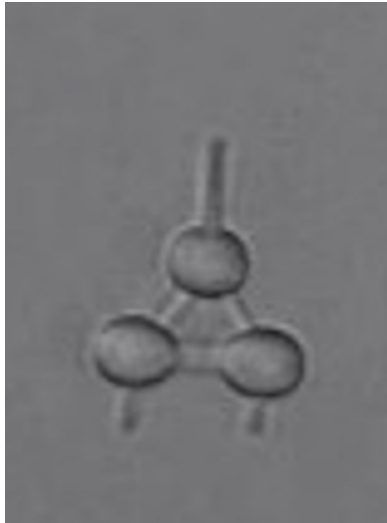


Figure 6. Manipulation of optically trapped probe produced using 2PP with movement in discrete steps (see movie 2, available from stacks.iop.org/NJP/12/113056/mmedia).

A likely explanation for the instability of the EBL probe is that it is due to its cylindrical trapping points (especially the edges of the cylinders). This produced distinct optical effects, as described in previous modeling work on the optical trapping of micron-sized cylinders using a laser beam with a focal spot size of $0.5 \mu\text{m}$ [14], and it was reported that such cylinders prefer to trap with the longest diagonal of the cylinders in parallel with the direction of propagation for the trapping laser beam. The preferred trapping orientation was prevented by the physical connection of the cylinders to the probe structure and resulted in an unbalanced set of trapping forces across the EBL probe structure. However, EBL probes with $4 \mu\text{m}$ size cylinders could be trapped (see figure 5) and this suggested that the destabilizing effects were sufficiently overcome at this size.

Each probe required precise adjustments to the three optical traps and beam-focusing optics to ensure that the probe was trapped parallel to the surface of the coverslip. These adjustments were observed using the CCD camera to image the three probe trapping points and when the trapping points were in a similar focus it was judged that the probe was parallel to the coverslip surface. The laser repositioning caused unwanted perturbations in the position of the rigid probe microstructure and this effect was found to be minimized by repositioning the laser beam at a rate of $\geq 40 \text{ kHz}$. The position of the probe within a ROI was calibrated by scanning the probe in two directions in steps of 40 nm across the ROIs. The probe was positioned at a height of $40 \mu\text{m}$ above the coverslip surface to avoid interference from the surface; all further tests were performed at this height. A linear range of position measurement was found for the EBL probe to be $\pm 0.44 \mu\text{m}$ from the center of the ROI in both directions, and $\pm 0.40 \mu\text{m}$ from the centre of the ROI for the 2PP probe. This difference was a result of the rounded appearance of the 2PP probe.

In order to derive the force applied to the probe, it was necessary to find the constant of proportionality that described the change in the probe's position in response to the force (as expressed by Hooke's law). This constant is known as the 'trap stiffness' and was calculated

Table 1. Trap stiffness measurements for the three cylindrical trapping points of the probe produced using EBL, normalized by optical power at the sample (153 mW).

	Probe point 1	Probe point 2	Probe point 3
Trap stiffness, x-direction ($\text{pN } \mu\text{m}^{-1} \text{ mW}^{-1}$)	0.041	0.036	0.034
Trap stiffness, y-direction ($\text{pN } \mu\text{m}^{-1} \text{ mW}^{-1}$)	0.065	0.062	0.054

Table 2. Trap stiffness measurements for the three spherical trapping points of the probe produced using two-photon polymerization, normalized by optical power at the sample (126 mW).

	Probe point 1	Probe point 2	Probe point 3
Trap stiffness, x-direction ($\text{pN } \mu\text{m}^{-1} \text{ mW}^{-1}$)	0.087	0.127	0.137
Trap stiffness, y-direction ($\text{pN } \mu\text{m}^{-1} \text{ mW}^{-1}$)	0.215	0.109	0.130

by using the equipartition method [25], which measured the probe's position change due to thermal effects (i.e. Brownian motion). Positional data were collected for 5 s at a rate of 15 kHz, and the variance was calculated for each probe-trapping point as it moved in two directions. Previous position measurements for a set of micrometer-sized spheres had shown ~ 1.5 nm rms accuracy [19]. The trap stiffness was found by dividing the position variance by the product of the Boltzmann constant and the temperature in kelvin (290 K at room temperature). The measurements for the EBL and 2PP probes are shown in tables 1 and 2, respectively.

The trap stiffness results for the spherical 2PP probe were 2–3 times greater than the results for the cylindrical EBL probe because of the 2PP probe's improved trapping stability provided by its rounded features, whereas the additional effects induced by the EBL probe's cylindrical trapping points are a likely cause for its reduction in trap stiffness, as discussed earlier.

In comparison with the shape of the EBL probe, the 2PP probe had an asymmetric distribution of material at its trapping points (see figure 6, with the $5 \mu\text{m}$ long tip connected to trapping point 1 and the remnants of the probe feet at trapping points 2 and 3) and we assume that this affected the distribution of the optical trapping forces and caused the variation in results shown in table 2. The majority of the trap stiffness results for the probes were smaller in comparison with the trap stiffness measurements made using the same instrumentation for one optically trapped sphere ($5.4 \mu\text{m}$ diameter polystyrene sphere; Interfacial Dynamics Corporation product no. 1-5000, batch no. 1089,1), which were $0.182 \text{ pN } \mu\text{m}^{-1} \text{ mW}^{-1}$ for the x-direction and $0.177 \text{ pN } \mu\text{m}^{-1} \text{ mW}^{-1}$ for the y-direction. This reduction is due to the method of trapping the probes (using multiple optical traps produced from one time-shared laser beam) leading to a reduction in optical power per trapping point.

Two further causes of trap stiffness variation for both types of probe were the limitations in dynamic response of the optical traps and their positioning relative to the probe's trapping points at each corner of the triangular probe. The positioning of the optical traps was performed manually by observing images of each trapped probe, as described earlier.

The bandwidth for probe force measurement was determined by calculating the power spectrum for each dimension of probe movement [25]. From this spectrum, a cut-off frequency

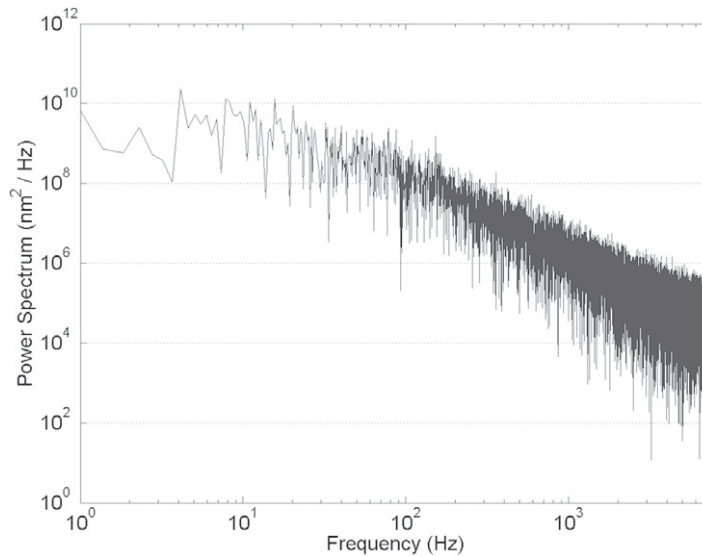


Figure 7. Power spectrum based on the positional data (y -direction, 5 s duration) of one trapping point on a probe produced using 2PP, showing the bandwidth of probe force measurement (30 Hz).

was found above which probe movements are attenuated. This behavior is typical of an optically trapped object and was confirmed for both types of probe, with the 2PP probe giving a force measurement bandwidth of 30 Hz, as demonstrated in the example power spectrum for one trapping point of a 2PP probe shown in figure 7.

The power spectrum measurement was used to confirm the trap stiffness measurement based on the equipartition method for the 2PP probe. The hydrodynamic drag coefficient (β) was calculated to be 1.01×10^{-7} , found by dividing the trap stiffness of the trapping point ($1.9 \times 10^{-5} \text{ N m}^{-1}$) by the cut-off frequency expressed as an angular frequency [25]. This value was in agreement with a value for β calculated by modeling the 2PP probe ($\beta = 1.12 \times 10^{-7}$) as the sum of three spheres of $4 \mu\text{m}$ diameter, where the motion of each sphere was described using Stoke's law [25].

3.2. Force measurement

We performed a force measurement experiment with a prototype EBL probe by applying a known force from a single optically trapped micro-sphere directly to the probe tip, as shown in figure 8. In this experiment, we used the optically trapped sphere purely for the purposes of calibration. The probe had a 200 nm wide tip made from SU8 and the microsphere had a diameter of $5.4 \mu\text{m}$ (the type of sphere was identical to that described in section 3.1). The probe and sphere were trapped simultaneously using four optical traps in total, with three traps used for the probe and one trap used for the sphere. The two objects were calibrated and trap stiffnesses were measured using the procedures described in section 3.1; the trap stiffness values in the direction of interest (the y -direction) were found to be $15.9 \text{ pN } \mu\text{m}^{-1}$ for the probe and $5.5 \text{ pN } \mu\text{m}^{-1}$ for the sphere.

To apply a force to the probe tip, the sphere was moved in the negative y -direction (see figure 8) towards the probe in steps of 40 nm over a total distance of $1.2 \mu\text{m}$. The sphere traveled

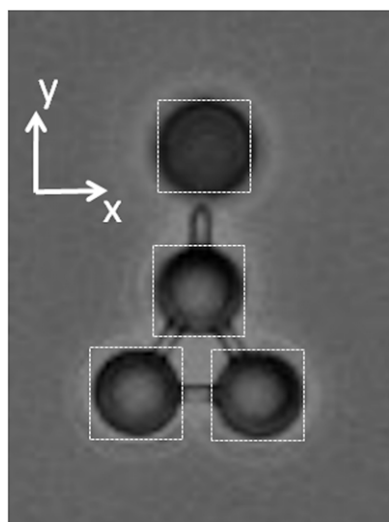


Figure 8. Experiment to apply a known force to the tip of an optically trapped EBL probe using an optically trapped sphere (top) in the y -direction as shown, with ROI locations shown by dotted white boxes where images of the probe corners and sphere were taken.

a distance of 500 nm before making contact with the probe tip and displaced each of the three probe trapping points, as shown at time = 4 s in figure 9(a). The maximum displacement of the probe was 134 nm, which corresponded to a displacement force of 2.13 pN using Hooke's law (this occurred at time = 8.25 s, with the displacement value relative to the displacement at time = 0 s). At the same time as contact was made, an unwanted displacement (average of 25 nm) was observed in the x -direction in probe trapping points 2 and 3, as shown in figure 9(b).

The force measured by the probe was compared to the restoring force exerted by the probe on the sphere. This force was calculated from the change in sphere displacement when contact was made with the probe and when the sphere was moved under control conditions without the presence of the optically trapped probe (see figure 10). The change in sphere displacement was 450 nm (occurring at time = 8.25 s), equal to a restoring force of 2.47 pN using Hooke's law.

The two force measurement values were different by 340 fN (13%) and this was linked to the displacement of two of the probe trapping points by 25 nm in the x -direction, corresponding to a force of \sim 400 fN. This shows that the direction in which force was applied by the sphere was not exactly perpendicular to the tip. It must be noted that the difference in force measurement is close to the minimum force that can be detected by the probe (240 fN rms), which is defined by the fluctuations in the probe position, measured from figure 9(a) to be 15.2 nm rms in the y -direction. The sphere's position fluctuations were measured to be 23.8 nm rms and this added the equivalent of 130 fN rms error to the restoring force measurement.

The fluctuations in sphere and probe positions were caused by thermally generated collisions with other particles in solution (Brownian motion). Control tests were carried out to determine the effect of moving the sphere and probe separately close to the trapping fields with no significant unwanted effects observed. The effect of moving the probe's tip into an optical field without a trapped sphere was also investigated and no significant perturbation to the probe was observed.

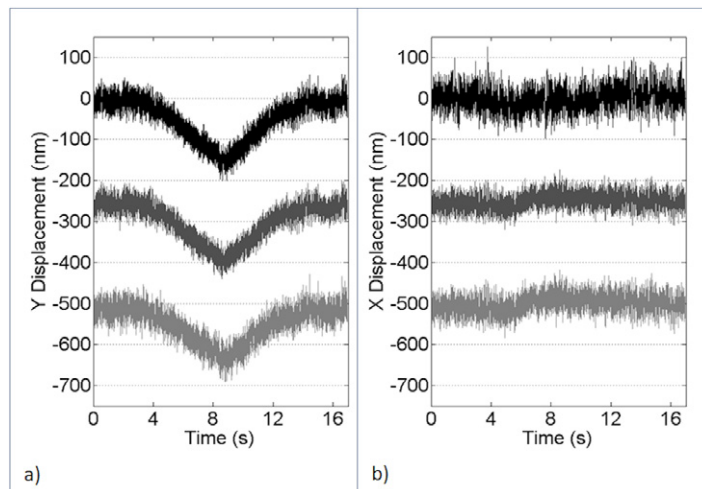


Figure 9. (a) Displacement of the three probe trapping points in the y -direction as the sphere applies force to the probe tip in the y -direction, making contact after 4 s. The plots are offset for clarity with probe trapping point 1 shown as the top trace, point 2 shown as the middle trace and point 3 shown as the bottom. (b) Displacements of probe trapping points in the x -direction under the same conditions.

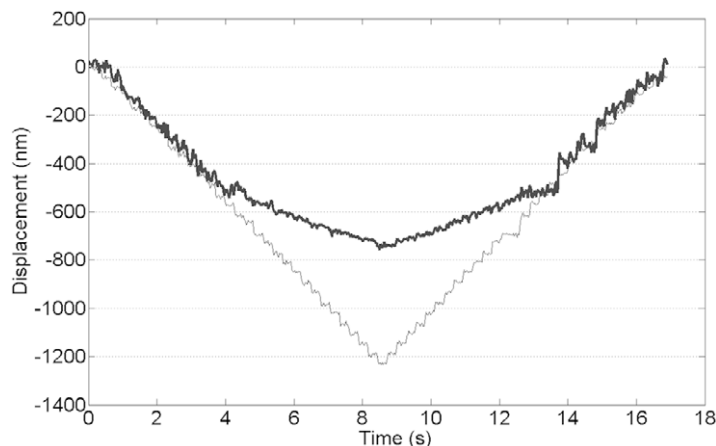


Figure 10. Movement of the optically trapped sphere when the probe and its trapping field are present (dark gray line) and not present (light gray line); note that the sphere appears to make contact with the probe tip after moving 500 nm (time = 4 s). Data points are averaged from 200 points of the original data set (250k points total sampled at 14.7 kHz).

The force measurement provided an independent confirmation of the trap stiffness measurement made earlier using the equipartition equation, which showed that the probe had a combined trap stiffness that was three times greater than the sphere's trap stiffness. This was a direct consequence of using a greater number of optical traps to trap the probe (three in total) compared to the sphere's one trap. The use of the equipartition equation was advantageous because it could calculate the probe's trap stiffness regardless of its physical complexity.

4. Conclusions

In conclusion, we have successfully developed an optically trapped probe that can measure forces via a protruding nanometer-sized tip. The probe's size and flexibility in rotation and translation offer the unique experimental capability of measuring forces on the transverse plane, which are distinct from uni-directional force measurement technologies such as atomic force microscopy [1]. Force measurements at the end of the tip along the probe's central axis were not significantly affected by the probe's trapping field, representing an improvement on force measurement using optically trapped spheres which cannot avoid the influence of the trapping field. The probe holds great promise as a platform to deliver a variety of molecular samples to biological systems (such as cells) and measure the interactions that occur. The ability to functionalize the probe with chemical samples is an important next step in experimental usage.

The change in probe manufacture that we have reported from EBL to 2PP has yielded probes with rounded features that have been trapped with greater ease and greater trap stiffness. The flexibility and precision of the 2PP process make it possible to produce probes with tip sizes as small as 30 nm [26] and of increasing complexity, permitting many variations of the probe to be produced. Optimization of the 2PP-produced probe is required in order to achieve symmetric distribution of the optical trapping forces.

A proposal for uni-directional force measurement using an optically trapped nano-tube has been made [9], believed to be accurate to 8 fN on a sub-millisecond time scale. In contrast, our probe demonstrated force measurement on a similar time scale to an accuracy of 240 fN over two directions. Moreover, our optically trapped probe has the unique advantage that it does not expose the sample directly to hazardous trapping light. The accuracy in our force measurement is limited by unwanted disturbance in the probe's position caused by Brownian motion. This disturbance can be reduced through the use of a feedback control system to readjust the positions of the optical traps based on probe displacement data [7, 27], which would utilize our FPGA electronics, APS and laser repositioning instrumentation. The implementation of this control system should improve the force measurement accuracy by at least an order of magnitude. Finally, the probe's performance can be further improved through optimization of the probe design, to reduce the trap stiffness variation between the three corners of the probe.

Acknowledgments

The instrumentation development was funded by the Science and Technology Facilities Council Technology Partnership (no. HC30202, 2005-8). We acknowledge the design and development of the 'Vanilla' active pixel sensor provided by MI3 Basic Technology Programme and STFC CMOS Sensor Design Group. We also acknowledge the significant contribution made to the development and production of the probes by Micro and Nanotechnology Centre at STFC (for electron beam lithography) and Laser Zentrum Hannover (for two-photon polymerization). The two-photon polymerization process was developed with financial support from the DFG Excellence Cluster 'Rebirth' and SFB Transregio 37. We thank Professor N Allinson (University of Sheffield) for PhD supervision of M R Pollard.

References

- [1] Neuman K C and Nagy A 2008 Single-molecule force spectroscopy: optical tweezers, magnetic tweezers and atomic force microscopes *Nat. Methods* **5** 491–505
- [2] Ashkin A, Dziedzic J M, Bjorkholm J E and Chu S 1986 Observation of a single-beam gradient force optical trap for dielectric particles *Opt. Lett.* **11** 288
- [3] Rohrbach A 2005 Switching and measuring a force of 25 femtoNewtons with an optical trap *Opt. Express* **13** 9695
- [4] Woodside M T, Anthony P C, Behnke-Parks W M, Larizadeh K, Herschlag D and Block S M 2006 Direct measurement of the full, sequence-dependent folding landscape of a nucleic acid *Science* **314** 1001
- [5] Svoboda K, Schmidt C F, Schnapp B J and Block S M 1993 Direct observation of kinesin stepping by optical trapping interferometry *Nature* **365** 721–7
- [6] Bormuth V, Varga V, Howard J and Schaffer E 2009 Protein friction limits diffusive and directed movements of kinesin motors on microtubules *Science* **325** 870
- [7] Molloy J E, Burns J E, Kendrick Jones, Tregear R T and White D C S 1995 Movement and force produced by a single myosin head *Nature* **378** 209–12
- [8] Selhuber-Unkel C, Zins I, Schubert O, Sonnichsen C and Oddershede L B 2008 Quantitative optical trapping of single gold nanorods *Nano Lett.* **8** 2998–3003
- [9] Marago O M, Jones P H, Bonaccorso F, Scardaci V, Gucciardi P G, Rozhin A G and Ferrari A C 2008 Femtonewton force sensing with optically trapped nanotubes *Nano Lett.* **8** 3211–16
- [10] Ashkin A and Dziedzic J M 1989 Optical trapping and manipulation of single living cells using infrared-laser beams *Ber. Bunsenges. Phys. Chem.* **93** 254–60
- [11] Ikin L, Carberry D M, Gibson G M, Padgett M J and Miles M J 2009 Assembly and force measurement with SPM-like probes in holographic optical tweezers *New J. Phys.* **11** 023012
- [12] Rodrigo P J, Kelemen L, Palima D, Alonzo C A, Ormos P and Glückstad J 2009 Optical microassembly platform for constructing reconfigurable microenvironments for biomedical studies *Opt. Express* **17** 6578
- [13] Galajada P and Ormos P 2003 Orientation of flat particles in optical tweezers by linearly polarized light *Opt. Express* **11** 446
- [14] Gauthier R C 1997 Theoretical investigation of the optical trapping force and torque on cylindrical micro-objects *J. Opt. Soc. Am. B* **14** 3323–33
- [15] Deufel C, Forth S, Simmons C R, Dejgoshia S and Wang M D 2007 Nanofabricated quartz cylinders for angular trapping: DNA supercoiling torque detection *Nat. Methods* **4** 223–5
- [16] Botchway S W, Towrie M and Ward A D 2006 Patent Number W0 2006/008550 ‘Optically Controllable Device’
- [17] Ovsianikov A, Gaidukeviciute A, Chichkov B N, Oubaha M, MacCraith B D, Sakellari I, Giakoumaki A, Gray D, Vamvakaki M, Farsari M and Fotakis C 2008 Two-photon polymerization of hybrid sol–gel materials for photonics applications *Laser Chem.* **2008** 493059
- [18] Guilford W H, Tournas J A, Dascula D and Watson D S 2004 Creating multiple time-shared laser traps with simultaneous displacement detection using digital signal processing hardware *Anal. Biochem.* **326** 153–66
- [19] Towrie M, Botchway S W, Clark A, Freeman E, Halsall R, Parker A W, Prydderch M, Turchetta R, Ward A D and Pollard M R 2009 Dynamic position and force measurement for multiple optically trapped particles using a high speed active pixel sensor *Rev. Sci. Instrum.* **80** 103704
- [20] Abbe E 1873 Beitrage zur Theorie des Mikroskops und der mikroskopsichen Wahrnehmung *Schultzes Arch. Mikr. Anat.* **9** 413–68
- [21] Mellor C D, Sharp M A, Bain C D and Ward A D 2005 Probing interactions between colloidal particles with oscillating optical tweezers *J. Appl. Phys.* **97** 103114
- [22] MI3 Basic Technology Programme website <http://mi3.shef.ac.uk> (accessed 2009)

- [23] Olivo A, Arvanitis C D, Bohndiek S E, Clark A T, Prydderch M, Turchetta R and Speller R D 2007 First evidence of phase contrast imaging with laboratory sources and active pixel sensors *Nucl. Instrum. Methods Phys. Res. A* **581** 776
- [24] Berry R and Burnell J 2001 *The Handbook of Astronomical Image Processing* (Richmond, VA: Willmann-Bell) p 185
- [25] Visscher K and Block S M 1998 Versatile optical traps with feedback control *Methods Enzymol.* **298** 460
- [26] Li L, Gattass R R, Gershgoren E, Hwang H and Fourkas J T 2009 Achieving $\lambda/20$ resolution by one-color initiation and deactivation of polymerization *Science* **324** 910–13
- [27] Wulff K D, Cole D G and Clark R L 2007 Servo control of an optical trap *Appl. Opt.* **46** 4923